1996ApJ...472L..49B

THE ASTROPHYSICAL JOURNAL, 472:L49–L52, 1996 November 20
© 1996. The American Astronomical Society. All rights reserved. Printed in U.S.A.

A λ = 1.3 MILLIMETER APERTURE SYNTHESIS MOLECULAR LINE SURVEY OF ORION KLEINMANN-LOW

GEOFFREY A. BLAKE,[1] L. G. MUNDY,[2] J. E. CARLSTROM,[3] S. PADIN,[3] S. L. SCOTT,[4] N. Z. SCOVILLE,[3] AND D. P. WOODY[4]
Received 1996 May 16; accepted 1996 September 6

ABSTRACT

We present a 1.″3 spatial resolution interferometric spectral line survey of the core of the Orion molecular cloud, obtained with the OVRO millimeter array. Covering 4 GHz bandwidth in total, the survey contains ∼100 emission lines from 18 chemical species. The spatial distributions of a number of molecules point to source I near the IRc2 complex as the dominant energy source in the region but do not rule out the presence of additional lower luminosity objects. At arcsecond resolution, the offsets between dust emission and various molecular tracers suggest that the spectacular "hot core" emission in the Orion core arises via the heating and ablation of material from the surfaces of very high density clumps located ≳500 AU from source I and traced by the dust emission. We find no evidence for a strong internal heating source within the hot core condensation(s).

Subject headings: ISM: individual (Orion Kleinmann-Low) — radio lines: ISM — techniques: interferometric

1. INTRODUCTION

The Orion KL region is one of the best studied areas of massive star formation in the Galaxy. Its close proximity and extraordinary brightness have enabled pioneering observations that, historically, have played a pivotal role in the understanding of more distant massive young stellar objects (YSOs; see Genzel & Stutzki 1989).

One of the first lessons learned was that massive stars form in complex environments. Early infrared (IR) studies revealed numerous objects, of which IRc2 and BN were identified as the main luminosity sources (Wynn-Williams et al. 1984), while molecular emission maps revealed a rich chemistry with kinematic variations that pointed to a wealth of unresolved substructure (Clark et al. 1976; Plambeck et al. 1982). The continued development of high angular resolution techniques in the IR and radio has led to ever more detailed images of Orion KL (Dougados et al. 1993; Menten & Reid 1995). With this perspective of 20 years experience, we can appreciate that the complexity of massive star formation regions is a necessary outcome of the gregarious and destructive nature of massive stars.

It is only recently that imaging at ≤1″ resolution has become possible at millimeter and submillimeter wavelengths (Lay et al. 1994; Sargent & Welch 1995; Wright, Plambeck, & Wilner 1996). In these regions, where previous spectral line survey work has been most rewarding (Johansson et al. 1984; Blake et al. 1987; Sutton et al. 1995), (sub)arc second imaging provides a unique view of the intimate association between the physical and chemical processes shaping the evolution of star-forming cores. This Letter presents the results of an interferometric survey of the dust and molecular emission from Orion KL in the λ = 1.3 mm atmospheric window. These data combine the high spatial resolution of other recent studies (Chandler & Depree 1995; Wright et al. 1995) with the great molecular complexity exhibited in line surveys of Orion KL, and provide interesting new constraints on the nature of this pivotal massive star forming cloud.

[1] Division of Geological and Planetary Sciences, California Institute of Technology, MS170-25, Pasadena, CA 91125; gab@gps.caltech.edu.
[2] Astronomy Department, University of Maryland, College Park, MD 20742; lgm@astro.umd.edu.
[3] Division of Physics, Mathematics & Astronomy, California Institute of Technology, MS 105-24, Pasadena, CA 91125.
[4] Owens Valley Radio Observatory, California Institute of Technology, Big Pine, CA 93513.

2. OBSERVATIONS

Observations of the Orion KL region at λ = 1.3 mm were carried out with the Owens Valley Radio Observatory (OVRO) millimeter array. Two local oscillator settings at 218.159 and 242.996 GHz were employed, with four separate digital correlator "stamps," each of width 240 MHz, covering the 1 GHz instantaneous IF bandwidth. The resulting spectra include a total of 3840 channels at a spectral resolution of 1 MHz.

The phase-tracking center for these observations was the brightest component of IRc2, $\alpha(1950) = 05^{h}32^{m}47^{s}.03$, $\delta(1950) = -05°24'23''.9$ (Gezari 1992; Dougados et al. 1993). Three transits with five telescopes were obtained at 218 GHz between 1993 November and 1994 February; two transits each in the five- and six-element arrays were obtained at 243 GHz between 1993 November and 1995 December. Raw visibility data were calibrated using the OVRO MMA software, with 0528+134 serving as the phase calibrator and 3C 273 and 3C 454.3 serving as the passband and secondary amplitude calibrators. Calibrated visibility data were then cleaned and mapped using MIRIAD. Unprojected baselines of 220 m N-S and 200 m E-W resulted in synthesized beams of 2″ × 1.″5 with natural weighting, and 1.″5 × 1.″0 with uniform weighting. At 218 and 243 GHz the primary beam of the 10.4 m telescopes is 30″ and 28″. The expected thermal noise limit of approximately 100–200 mJy beam^{-1} per 1 MHz channel is rarely reached in the maps due to the equatorial declination of Orion, which causes scattered flux from the shorter baselines to dominate the rms noise.

3. RESULTS AND DISCUSSION

Spectra of the frequency ranges covered in the OVRO λ = 1.3 mm survey are presented in Figure 1. These frequency windows were selected to provide images of a wide range of different molecules and excitation mechanisms. A pseudo-continuum channel was generated by binning together groups of channels free of obvious line emission. Nearly 100 spectral lines from some 18 molecules are evident. We discuss below the dust continuum images and, in turn, a small selection of

© American Astronomical Society • Provided by the NASA Astrophysics Data System

1996ApJ...472L..49B

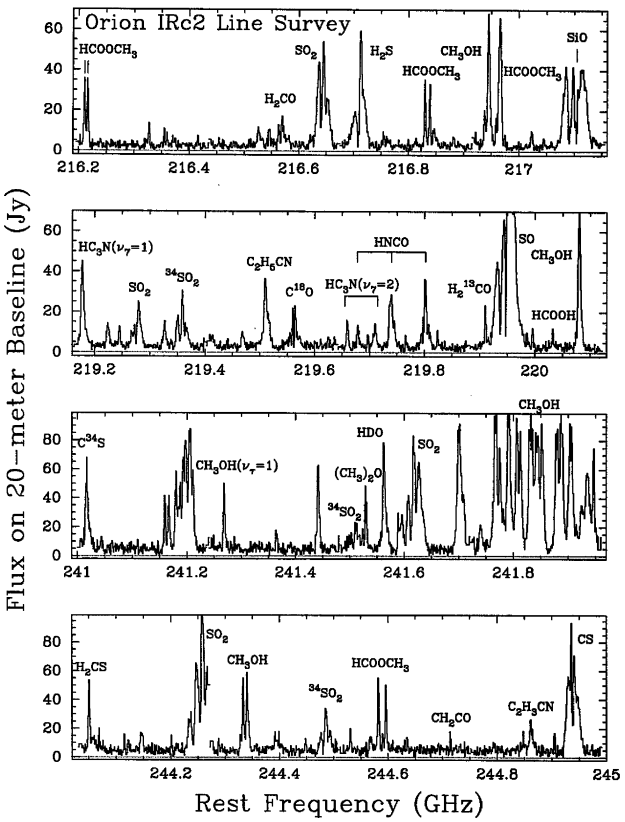

FIG. 1.—Overview of the OVRO $\lambda = 1.3$ mm interferometric spectral line survey of Orion KL. The spectra presented are the track-averaged emission from the phase tracking center on a single 20 m E-W baseline. The spectral resolution is 1 MHz, the flux scale is in Jy. Selected transitions from the 18 species detected in the survey are labeled for clarity. The offset in the spectrum is due nearly entirely to dust continuum emission.

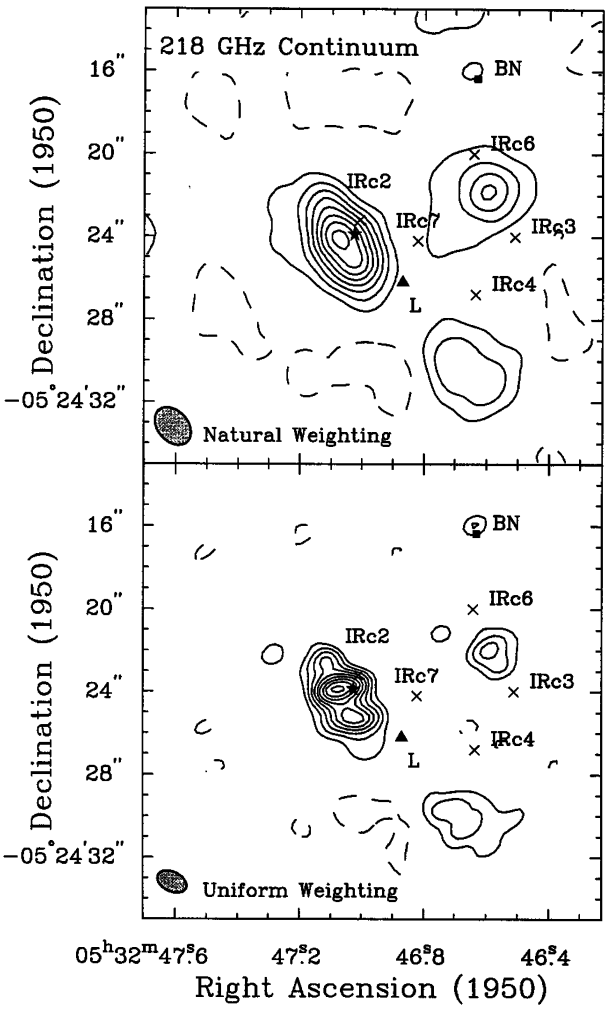

FIG. 2.—OVRO 218 GHz continuum maps of the Orion KL region, formed from "line-free" regions of the survey depicted in Fig. 1. *Top*, naturally weighted image, beam size = 2.″1 × 1.″5, contour interval 100 mJy beam^{-1} (~1 K), starting at 100 mJy beam^{-1}. *Bottom*, uniform-weighted image, beam size = 1.″5 × 1.″0, contour interval 50 mJy beam^{-1} (~1 K), also beginning at 100 mJy beam^{-1}. In each panel, the location of BN is depicted with a solid square, radio source I and SiO maser position as a solid star, and radio source L (source *n* in Menten & Reid 1995) as a solid triangle. Several of the additional infrared sources in this region are indicated as crosses. From top to bottom, the detected sources can be associated with the northwest clump (NW), hot core (HC), and compact ridge (CR) regions identified by previous workers.

spectral line maps. A more exhaustive presentation of the line survey results and images will be presented elsewhere (Blake et al. 1996).

3.1. *Dust Continuum Emission*

Figure 2 presents both natural- and uniform-weighted images of dust emission near 218 GHz.[5] The 218 and 243 GHz maps are similar in many respects to previous $\lambda = 3$ mm images (Masson & Mundy 1988; Wright et al. 1992; Murata et al. 1992; Plambeck et al. 1995), but do not require the subtraction of free-free emission from the overlying H II region. All three prominent sources seen previously, corresponding to the hot core (HC) near IRc2, the northwest clump (NW) between IRc 3 and IRc 6, and the compact ridge (CR) south of IRc 4, are clearly detected. BN is also weakly visible to the north.

At uniform-weighted resolution (1.″5 × 1.″0), the HC breaks up into two, or perhaps three, sources. Both the peak and total fluxes are very sensitive to resolution, since there is substantial emission on scales larger than those sampled by the array. A fair comparison can be made between our data and those of Plambeck et al. (1995) at 1.″2 resolution. The peak fluxes (66 mJy beam^{-1} at $\nu = 86.2$ GHz; 520 mJy beam^{-1} at $\nu = 218$ GHz) yield a HC spectral index ($F_\nu \propto \nu^\alpha$) of 2.2 ± 0.3.

[5] FITS images of the maps shown in this paper may be obtained at URL http://imagelib.ncsa.uiuc.edu.

The NW and CR clumps are not detected at $\lambda = 3$ mm (<8 mJy beam^{-1}, 4 σ) so we can only derive lower limits of $\alpha > 3.6$ and $\alpha > 3.4$. Our spectral index for the HC differs significantly from that derived by Wright et al. (1992), probably due mainly to the difference in resolution. Further investigation of dust emissivity variations will require more detailed source structure and opacity models.

As Figure 2 shows, there is a marked anticorrelation between the $\lambda = 1.3$ mm and IR emission at ~1″ resolution. Using a mass opacity coefficient of $\kappa_\nu(1.3\ \mathrm{mm}) = 0.019$ g cm^{-2} (the 250 μm emissivity of Hildebrand 1983 and $\alpha = 3$) and $T_{\mathrm{dust}} = 100$ K yields peak masses, column densities, and densities of 0.25 $M_\odot$, 1×10^{24} cm^{-2}, and 2×10^8 cm^{-3} for the brightest clumps in Figure 2b; the density was calculated assuming a spherical, constant-density source (a spectral index

© American Astronomical Society • Provided by the NASA Astrophysics Data System

1996ApJ...472L..49B

of $\alpha = 4$ would raise these estimates by ~5). The total mass in this map is $\leq 1\ M_\odot$, quite a bit less than the $\sim 10\ M_\odot$ found on 4″–10″ scales by Masson & Mundy (1988). Peak column densities are nearly identical, however. In effect, we are sensitive to only the most compact components of the dust distribution. Despite their small masses, the far- and mid-IR opacities of the dust sources are quite high, reaching $\tau \sim 5$–10 at $\lambda = 30\ \mu$m, thus explaining the observed millimeter/IR anticorrelation.

We find, as have other recent studies (Menten & Reid 1995; Chandler et al. 1996; Plambeck et al. 1995), that IRc2 and source I are offset from the HC, as defined by the dust continuum emission. These investigators have also determined that source I, which is centered within the SiO($\nu = 1$) maser ring, not IRc2, is the true center of energetic behavior in the Orion core. Our upper limit to the source I pointlike flux constrains the dust + gas mass at this position to $\leq 0.3\ M_\odot$, in agreement with Plambeck et al. (1995). Like the latter authors, we do not detect radio source *n* (Menten & Reid 1995).

3.2. *Molecular Line Emission*

The line-of-sight distances from the HC continuum peaks to source I are ~500–750 AU, suggesting that they are externally heated. One might expect the resulting energy density gradient to be reflected in the excitation and emission distributions of various molecules, and rotational temperatures from 90 to 400 K are in fact observed for molecules with HC line shapes (Genzel & Stutzki 1989). The overall placement of the clumps, the velocity field of the SiO masers, and the blueshifted velocity of high excitation HC emission suggest a causal relationship in which source I lies behind the dense clumps and evaporates or ablates them by a combination of an intense radiation field and a poorly collimated wind. Simple consideration of such a scenario predicts that the highest excitation tracers should be anticorrelated with millimeter-wave emission from cool dust.

It is not possible to present herein all of the emission distributions observed. Figure 3 (Plate L7) presents an overview of the velocity-integrated emission from six species, SiO, C_2H_5CN, HC_3N, HNCO, $HCOOCH_3$, and HDO, overlayed on the uniform-weighted dust emission image. Critical densities and level energies for most of the transitions presented in Figure 1 lie in the 10^{6-7} cm^{-3}, 100–500 K range, and so the OVRO survey preferentially samples emission from compact regions of warm, dense gas. Peak brightness temperatures in Figure 3 range from 15 K for HDO to 95 K for SiO. Individual channel maps of each species have peak temperatures that are 2–3 times higher, implying optical depths near unity. Each species is discussed in greater detail below.

3.2.1. SiO $J = 5 \rightarrow 4$

Silicon is known to be strongly depleted in dense, quiescent gas. Regions of intense SiO emission preferentially trace energetic processes which cause grain, or grain mantle, sputtering (Wright et al. 1983; Bachiller & Gomez-Gonzalez 1992). Recent imaging by Chandler et al. (1996) and Wright et al. (1995) has shown that the lowest transitions of SiO are masing even in the ground vibrational state ($T_B \sim 10^5$ K at $J = 1 \rightarrow 0$, 2000–3000 K at $J = 2 \rightarrow 1$), and that the degree of masing drops rapidly with J. By $J = 5 \rightarrow 4$ the observed brightness temperature has dropped to ~100 K in the OVRO 1.″5 beam, constraining the density in the $\nu = 0$ masing region to be $\leq 10^7$ cm^{-3} (Zeng, Sun, & Lou 1987).

The observed morphology is similar to that seen by Chandler et al. (1996) and Wright et al. (1995), with an elongated emission region centered just north of source I (i.e., away from the HC) and roughly perpendicular to the axis of shocked molecular hydrogen. At the ends of the SiO outflow, the emission contours turn approximately E-W in a fashion that avoids the regions traced by the $\lambda = 1.3$ mm continuum. The broad line wings observed in SiO strongly suggest that destructive shock sputtering and shattering of grains is responsible for the enhanced silicon gas phase abundance, naturally explaining the observed anticorrelation with the high-density peaks traced by the dust emission.

3.2.2. *Vibrationally Excited* HC_3N *and High-*K HNCO

Molecules whose excitation is dominated by photon pumping at IR wavelengths offer a means of imaging the infrared radiation environment at high angular resolution. Since direct imaging of the far-IR radiation field at arcsecond resolution is not currently feasible, such molecules are unique probes of the radiation environment deep inside molecular clouds. Maps of two infrared-sensitive transitions are presented in Figure 3.

The first, the $\nu_7 = 1$ excited bending state of HC_3N, requires photons near $\lambda = 45\ \mu$m. Cyanoacetylene is a widespread interstellar molecule, and within Orion KL itself HC_3N shows all of the distinct kinematic signatures (ridge, hot core, and plateau). The second molecule is isocyanic acid, HNCO. Its $K_p = 1$, 2, 3, and 4 stacks are connected to each other via *b*-dipole transitions lying near 320, 80, 35, and 20 μm, respectively (Churchwell et al. 1986). Each of these stacks has transitions in the survey, here we present a $K_p = 2$ transition to probe longer wavelengths ($\lambda = 80\ \mu$m) than those required for HC_3N.

The HC_3N/HNCO distributions presented in Figure 3 are similar, but not identical. In each case, the emission peaks close to source I, but is coincident neither with source I, IRc2, *or* the peaks of the dust distribution. While the clumps closest to source I are quite similar in HC_3N and HNCO, on average the HNCO clumps lie at a greater distance, reflecting a softening of the radiation field with increasing extinction. Where the emission differs most is in the southwestern tongue; HC_3N projects directly toward IRc 4, whereas HNCO tends to avoid this region. This same morphology is observed in the other HNCO transitions, and suggests that chemistry not excitation is responsible for the difference.

3.2.3. HDO, C_2H_5CN, *and* $HCOOCH_3$

Current models of the chemistry of hot cores rely greatly on the interaction of gas and dust (see Charnley, Tielens, & Millar 1992; Caselli, Hasegawa, & Herbst 1993). Three kinds of molecules can be distinguished in these models: those species passively trapped in grain mantles and released chemically unaltered by heating once star formation occurs; those synthesized actively on dust grains and then desorbed by high-temperature processes; and those created in the gas phase by combination of ion-molecule and neutral chemistry in the hot core *after* mantle evaporation. Here, we use HDO, C_2H_5CN, and $HCOOCH_3$, respectively, as molecules sensitive to these three different formation routes.

As might be expected from the complex processes at work, striking differences in the emission patterns are observed

© American Astronomical Society • Provided by the NASA Astrophysics Data System

1996ApJ...472L..49B

© American Astronomical Society • Provided by the NASA Astrophysics Data System

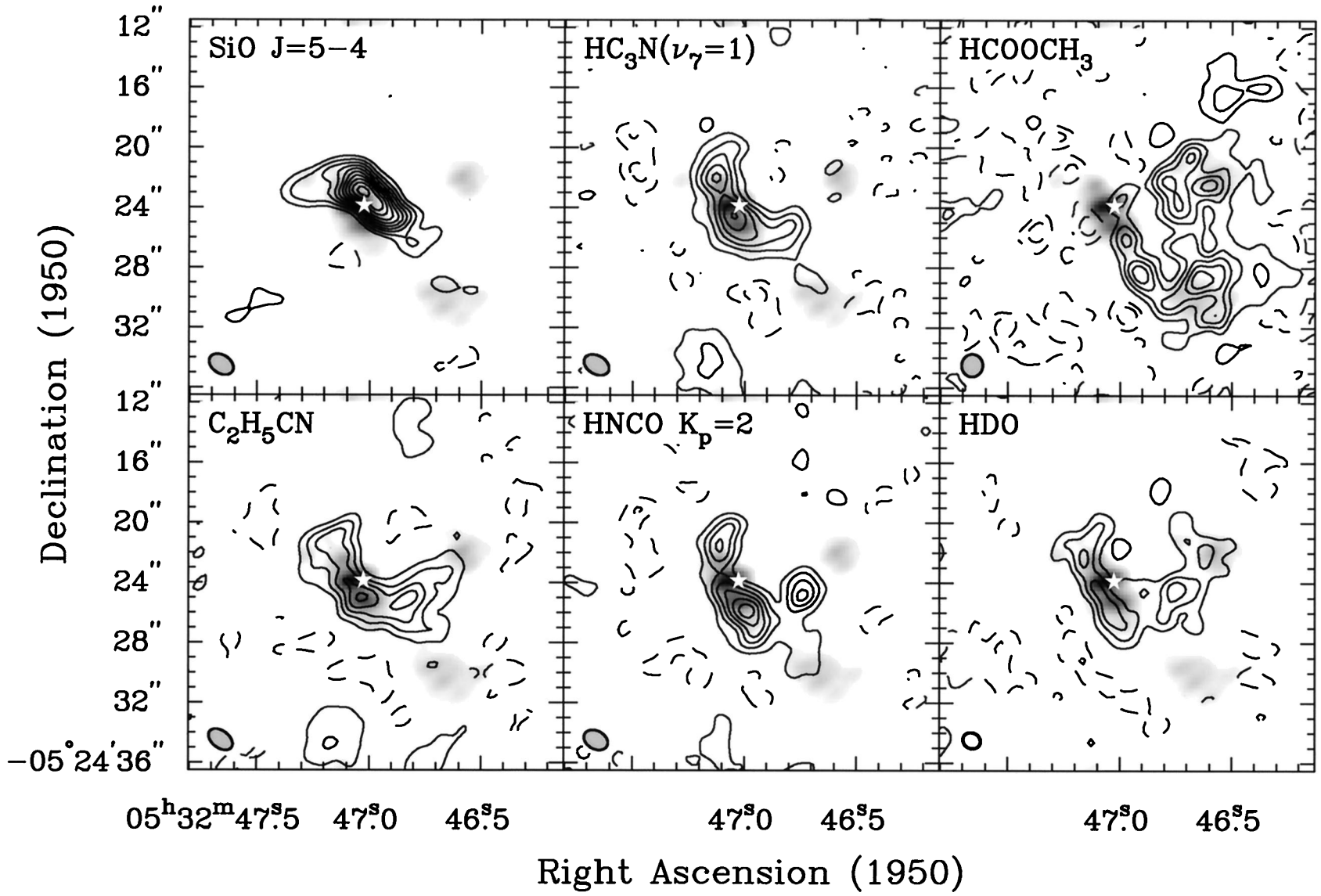

FIG. 3.—Multipanel image summarizing various aspects of the chemistry observed toward Orion KL (IRc2 region) at $\lambda = 1.3$ mm. In each panel, the gray scale presents the uniform-weighted dust continuum emission (see Fig. 2, bottom) at $1\farcs5 \times 1\farcs0$ resolution. The contours depict the uniform-weighted maps obtained for selected molecules, noted in the upper left hand corner of each panel. Contour levels for the $HCOOCH_3$ $J_{K_p K_o} = 20_{4,17} \rightarrow 19_{4,16}$ A transition are spaced by 0.6 Jy beam^{-1} (6 K), those for SiO $J = 5 \rightarrow 4$ at 0.5 Jy beam^{-1} (8 K), those for HDO $J_{K_p K_o} = 2_{11} \rightarrow 2_{12}$ and HNCO $J_{K_p K_o} = 10_{29} \rightarrow 9_{28}$ at 0.4 Jy beam^{-1} (4 and 7 K), and those for $HC_3N(\nu_7 = 1)$ $J = 24 \rightarrow 23$ ($1f$) and C_2H_5CN $J_{K_p K_o} = 24_{2,22} \rightarrow 23_{2,21}$ at 0.3 Jy beam^{-1} (5 K); contouring begins at the step level in each case. The white star marks the position of radio source I and the SiO($\nu = 1$) maser ring.

1996ApJ...472L..49B

which reflect diverse physical and chemical histories of the gas on small spatial scales. In each case, the emission is anticoincident with the dust peaks, not surprising in light of the high optical depths in these clumps to radiation at wavelengths short enough to heat the gas. C_2H_5CN has a shape which is closest to that of the "traditional" HC observed at lower resolution (see Masson & Mundy 1988).

HDO also has a HC line shape, and while the overall morphology is similar to that of C_2H_5CN and $HC_3N(\nu_7 = 1)$ (see also Plambeck & Wright 1987), a closer inspection of Figure 3 revels that the peaks in the HDO distribution are offset slightly from these two species—generally in a fashion that places the HDO emission at slightly further projected distances from IRc2/source I. Densities of order 10^9 cm^{-3} are required to thermalize HDO, and so pumping by far-IR and *submillimeter* photons are also likely—again suggesting a reddening of the radiation field with distance from source I.

This trend is continued in the emission from torsionally excited CH_3OH, which has strong peaks near all the dust clumps and is dramatically outlined by $HCOOCH_3$ for which only a small tongue of emission at the bluest velocities appears near the HC. Most of the $HCOOCH_3$ emission arises near the CR and NW clumps in patterns that avoid the strongest HDO peaks. Similar features are observed in other complex, oxygen-containing species such as $(CH_3)_2O$, and are also seen in H_2CS and H_2CO. In each case, the bulk of the emission is centered close to the NW or CR clump, on the side *toward* source I. Such relationships among the more complex molecules are predicted by ion-molecule reaction networks (Charnley et al. 1992), chemistry not favored by the high densities and temperatures near the HC. Thus, the observed spatial patterns strikingly confirm the kinematic distinctiveness of the HC and CR (see Johansson et al. 1984; Blake et al. 1987), and suggest that variations in both the physical conditions and grain mantle composition play important roles in the chemical evolution of the Orion core.

4. SUMMARY AND CONCLUSIONS

The observed peaks in both dust and line emission are consistent with source I providing most of the luminosity in Orion KL, but the data do not rule out contributions from other moderate luminosity sources that are almost certain to be present. All tracers of activity suggest that strong excitation gradients exist, with the highest energy density lying near source I. It is here where the most tightly bound grain mantle constituents are found in the gas phase, and where molecules subsequently formed by neutral-neutral chemistry—which is potentially much more sensitive to reaction barriers than ion-molecule chemistry—dominate. Further from source I, but near the compact ridge and north west clump dust peaks, more fragile (H_2CO or H_2CS) and/or more complex molecules formed by ion-molecule reactions [$HCOOCH_3$ or $(CH_3)_2O$] are found.

Unlike most previous work at coarser spatial resolution, we find the dust and gas tracers to be strongly anticorrelated at 1″ scales. Taken together, the observed "limb-brightened" distributions and the chemical properties are consistent with the dominant role of the source I/IRc2 complex coupled with the effects of extinction (see Wynn-Williams et al. 1984). The dust morphology and molecular kinematics suggest that source I lies close to and behind the dense clumps, whose exteriors are currently being evaporated and/or ablated. In effect, these cool cores serve as reservoirs for the chemically and spectrally rich hot core phase of massive star formation first recognized in Orion, and help to maintain it for the $\sim 10^{4-5}$ years required for the chemistry to reach the observed level of complexity.

Furthermore, the reddening of the source I radiation field with distance may lead to efficient heating of the clump exteriors in "cool" photon dominated regions similar to those recently proposed to exist around low-mass YSOs (Spaans et al. 1995) but not to extensive dissipation of the dense gas, naturally forming the warm cocoons of gas that may help resolve the lifetime paradox associated with ultracompact H II regions (Depree, Rodriguez, & Goss 1995). Such cores may harbor low- to moderate-mass stars, or might well form them in the absence of their more destructive cousins, but we find no evidence that they are currently being heated from within.

Millimeter interferometry at OVRO is supported by the NSF, grant AST-9314079. G. A. B. would like to acknowledge additional support from NASA, grants NAGW-1955 and NAGW-2297, while L. G. M. acknowledges support from NSF grant AST-9314847 and NASA grant NAGW-3066. J. E. C. acknowledges support from the NSF-YI program and the David & Lucille Packard Foundation. L. G. M. and G. A. B. gladly thank Leiden Observatory for their hospitality during the course of this work.

REFERENCES

Bachiller, R., & Gomez-Gonzalez, J. 1992, Astron. Astrophys. Rev., 3, 257
Blake, G. A., Sutton, E. C., Masson, C. R., & Phillips, T. G. 1987, ApJ, 315, 621
Blake, G. A., et al. 1996, in preparation
Caselli, P., Hasegawa, T. I., & Herbst, E. 1993, ApJ, 408, 548
Chandler, C. J., et al. 1996, ApJ, submitted
Chandler, C. J., & Depree, C. G. 1995, ApJ, 455, L67
Charnley, S. B., Tielens, A. G. G. M., & Millar, T. J. 1992, ApJ, 399, L71
Churchwell, E., Wood, D., Myers, P. C., & Myers, R. V. 1986, ApJ, 305, 405
Clark, F. O., Brown, R. D., Godfrey, P. D., Storey, J., & Johnson, D. 1976, ApJ, 210, L139
Depree, G. G., Rodriguez, L. F., & Goss, W. M. 1995, Rev. Mexicana Astron. Astrofis., 31, 39
Dougados, C., Léna, P., Ridgway, S. T., Christou, J. C., & Probst, R. G. 1993, ApJ, 406, 112
Genzel, R., & Stutzki, J. 1989, ARA&A, 27, 41
Gezari, D. Y. 1992, ApJ, 396, L43
Hildebrand, R. H. 1983, QJRAS, 24, 267
Johansson, L., Andersson, C., Ellder, J, Friberg, P., & Hjalmarson, A. 1984, A&A, 130, 227
Lay, O. P., Carlstrom, J. E., Hill, R. E., & Phillips, T. G. 1994, ApJ, 434, L75
Masson, C. R., & Mundy, L. G. 1988, ApJ, 324, 538
Menten, K. M., & Reid, M. J. 1995, ApJ, 445, L157
Murata, Y., Kawabe, R., Ishiguro, M., Morita, K., Hasegawa, T., & Hayashi, M. 1992, PASJ, 44, 381
Plambeck, R. L., & Wright, M. C. H. 1987, ApJ, 317, L101
Plambeck, R. L., Wright, M. C. H., Mundy, L. G., & Looney, L. W. 1995, ApJ, 455, L189
Plambeck, R. L., Wright, M. C. H., Welch, W. J., Bieging, J. H., Baud, B., Ho, P., & Vogel, S. N. 1982, ApJ, 259, 617
Sargent, A. I., & Welch, W. J. 1995, ARA&A, 31, 297
Spaans, M., Hogerheijde, M. R., Mundy, L. G., & van Dishoeck, E. F. 1995, ApJ, 455, L167
Sutton, E. C., Peng, R., Danchi, W. C., Jaminet, P. A., Sandell, G., & Russell, A. P. G. 1995, ApJ, 97S, 455
Wright, M. C. H., Plambeck, R. L., Mundy, L. G., & Looney, L. W. 1995, ApJ, 455, L185
Wright, M. C. H., Plambeck, R. L., Vogel, S. N., Ho, P., & Welch, W. J. 1983, ApJ, 267, L41
Wright, M. C. H., Plambeck, R. L., & Wilner, D. J. 1996, ApJ, 469, 216
Wright, M. C. H., Sandell, G., Wilner, D. J., & Plambeck, R. L. 1992, ApJ, 393, 225
Wynn-Williams, C. G., Genzel, G., Becklin, E. E., & Downes, D. 1984, ApJ, 281, 172
Zeng, Q., Sun, J., & Lou, G. F. 1987, A&A, 172, 299

© American Astronomical Society • Provided by the NASA Astrophysics Data System